Journal of Controlled Release 187 (2014) 145–157

Contents lists available at ScienceDirect

Journal of Controlled Release

journal homepage: www.elsevier.com/locate/jconrel

Anticancer polymeric nanomedicine bearing synergistic drug combination is superior to a mixture of individually-conjugated drugs

Ela Markovsky [1], Hemda Baabur-Cohen [1], Ronit Satchi-Fainaro *

Department of Physiology and Pharmacology, Sackler School of Medicine, Tel Aviv University, Tel Aviv 69978, Israel

ARTICLE INFO

Article history:
Received 4 February 2014
Accepted 16 May 2014
Available online 24 May 2014

Keywords:
Cancer treatment
Polymeric nanomedicines
Combination therapy
Polyglutamic acid
Chemotherapy
Drug-polymer conjugates

ABSTRACT

Paclitaxel and doxorubicin are potent anticancer drugs used in the clinic as mono-therapies or in combination with other modalities to treat various neoplasms. However, both drugs suffer from side effects and poor pharmacokinetics. These two drugs have dissimilar physico-chemical properties, pharmacokinetics and distinct mechanisms of action, toxicity and drug resistance. In order to target both drugs selectively to the tumor site, we conjugated them at a synergistic ratio to a biocompatible and biodegradable polyglutamic acid (PGA) backbone. Drugs conjugation to a nano-sized polymer enabled preferred tumor accumulation by passive targeting, making use of the enhanced permeability and retention (EPR) effect. The rational design presented here resulted in co-delivery of combination of the drugs and their simultaneous release at the tumor site. PGA–paclitaxel–doxorubicin nano-sized conjugate exhibited superior anti-tumor efficacy and safety compared to the combination of the free drugs or a mixture of the drugs conjugated to separate polymer chains, at equivalent concentrations. This novel polymer-based multi-drug nano-sized conjugate allowed for true combination therapy since it delivered both drugs to the same target site at the ratio required for synergism. Using mice bearing orthotopic mammary adenocarcinoma, we demonstrate here the advantage of a combined polymer therapeutic bearing two synergistic drugs on the same polymer backbone, compared to each drug bound separately to the backbone.

1. Introduction

The conjugation of anticancer drugs with biocompatible polymers offers many advantages over small molecular therapeutics. These include: (i) improved solubility and stability, (ii) preferred passive accumulation of the drug at the tumor site by the enhanced permeability and retention (EPR) effect [1,2], (iii) reduced systemic toxicity and decreased or even abrogated immunogenicity, (iv) ability to overcome cancer cells resistance, and (v) increased therapeutic efficacy [3]. Many of the above advantages arise from the nano-scaled size of the polymer therapeutic. The high molecular-weight nanocarrier can only extravasate through the leaky blood vessels at the tumor area and internalize into target cells via endocytosis, resulting in a longer circulation time of the conjugate in the bloodstream compared with the free drugs [3]. This phenomenon of passive diffusion through the hyperpermeable neovasculature and localization in the tumor interstitium is observed in many solid tumors for macromolecular agents and lipids [4]. Currently, a number of polymer–drug conjugates are available for cancer treatment, and more are in the pipeline for clinical studies [5,6].

Another advantage of polymeric nanomedicines is their versatility, enabling to tailor different compounds with controlled loading percentage on a single polymeric backbone [7,8]. This property can be utilized for the coupling of two chemotherapeutic drugs, with different mechanisms of action, and different resistance and toxicity profiles, on the same nanocarrier. Importantly, coupling two agents that act synergistically will allow the administration of lower concentrations of each agent, increasing their combined anti-tumor efficacy and decreasing their toxicity. These multivalent polymeric nanocarriers serve as ideal platforms for true combination therapy, where the therapeutics are given simultaneously in one injection and share the same pharmacokinetic profile [9–11].

The anthracycline antibiotic, doxorubicin (DOX) and the microtubule-interfering agent, paclitaxel (PTX), are clinically well-established and highly effective anti-neoplastic medications as mono-therapies [12,13] and as sequential combination therapy [14–17]. As small Mw agents, they both suffer from different side effects, like neurotoxicity for PTX and cumulative dose-related cardiotoxicity for DOX [18]. Furthermore, since PTX is not water-soluble, it is administered with a solubilizing agent cremophor EL, which causes hypersensitivity reactions by itself [19].

A chemical conjugation of PTX and DOX to a nanocarrier could offer pharmacodynamic and pharmacokinetic advantages by passively targeting both drugs to the tumor site at the required ratio for synergism. Polyglutamic acid (PGA) is a water-soluble multivalent

* Corresponding author. Tel.: +972 3 640 7427; fax: +972 3 640 9113.
E-mail address: ronitsf@post.tau.ac.il (R. Satchi-Fainaro).
[1] These authors contributed equally to this work.

http://dx.doi.org/10.1016/j.jconrel.2014.05.025
0168-3659/

polymer which allows the conjugation of several compounds or targeting moieties within the polymer backbone [20–22]. It is non-immunogenic, is non-toxic, and is biodegradable by cathepsin B, an enzyme that is highly expressed in most tumor tissues [23–26]. PGA enables multivalent binding of synergistic drugs and selective delivery to tumors when used at an appropriate nano-scaled size. Those features make PGA an attractive drug carrier. Indeed, PGA–PTX (OPAXIO™) is currently being evaluated in Phase III clinical trials for ovarian cancer as a single agent [27,28], and for non-small-cell lung cancer in combination with carboplatin [29]. A Phase III clinical trial was recently concluded for OPAXIO™ as an orphan drug in combination with temozolomide and radiotherapy for patients suffering from glioblastoma multiforme (GBM) [30]. OPAXIO™ could not be safely combined with temozolomide due to Grade 4 hematologic toxicity. However, the favorable progression-free and overall survival suggested that OPAXIO™ may enhance radiation for GBM [30]. It is increasingly clear that combination therapy is likely to provide a long-term solution for the treatment of metastatic and/or resistant disease. Recently, several studies have explored the advantage of using a combination therapy in polymer–drug conjugates [31–35].

The aim of this study was to synthesize a polymer therapeutic combining two synergistic drugs on the same polymer chain at an appropriate ratio, and to determine its *in vivo* advantage over drugs conjugated to separate polymer chains and to free drugs.

2. Materials and methods

2.1. Ethics statement

All animal procedures were performed in compliance with Tel Aviv University guidelines approved by the Institutional Animal Care and Use Committee.

2.2. Materials

All chemicals and solvents were A.R. or HPLC grade. Chemical reagents were purchased from Sigma-Aldrich (Israel) and Merck (Israel). HPLC grade solvents were purchased from Biolab (Israel). Paclitaxel and doxorubicin hydrochloride were purchased from Petrus Chemicals and Materials Ltd. (Israel). All tissue culture reagents were purchased from Biological Industries Ltd (Beit Haemek, Israel), unless otherwise indicated. PGA was purchased from Alamanda Polymers (Huntsville, AL, USA).

2.3. Chemical data

All reactions requiring anhydrous conditions were performed under a nitrogen atmosphere. Size exclusion chromatography (SEC) analysis was performed using UltiMate 3000 LC System (Thermo Scientific) with photodiode array (PDA)-UV detector and Shodex RI-101 detector (Showa Denko America, Inc.), with Zenix SEC-100 (Sepax) column in phosphate buffer pH = 7.0, flow 1 ml/min. Reversed phase (RP) high pressure liquid chromatography (HPLC) analysis was performed using UltiMate 3000 LC system (Thermo Scientific) with PDA-UV detector and C18 LiChroCART® Purospher® STAR250 × 4.6 mm column (5 μm) (Merck Millipore). The mobile phase was a gradient of water (A) and acetonitrile (ACN) (B) both containing 0.1% (vol/vol) trifluoroacetic acid (TFA), 20% to 100% solvent B in 15 minutes. Chromelion software was employed for data analysis. Polymer conjugates were purified by SEC on Sephacryl S-200 HR (GE Healthcare, Buckinghamshire, UK), using water as eluent. Chemical reagents included: *N*, *N*-diisopropylcarbodiimide (DIC), 1-hydroxybenzotriazol (HOBt), diisopropylethylamine (DIPEA), *N*-hydroxysuccinimide (OHSuc), *N*,*N*-dimethylaminopyridine (DMAP), anhydrous *N*,*N*-dimethylformamide (DMF), and anhydrous tetrahydrofuran (THF).

2.4. Synthesis of PGA–PTX–DOX

In this combined conjugate PTX is bound directly to the PGA by an ester bond and DOX is bound through an acid-sensitive hydrazone bond. PGA–PTX–DOX conjugate was synthesized using the following steps (Scheme 1):

2.4.1. Synthesis of PGA–PTX

PTX (29.7 mg, $3.48 * 10^{-2}$ mmol) was conjugated to PGA (150.0 mg, 1.16 mmol; 100 units, Mw ~13 kDa) by carbodiimide coupling (DIC/HOBt) in anhydrous DMF (10 ml). After 24 hours the solvent was evaporated under high vacuum and the residue washed in chloroform/acetone (4:1). The resulting precipitate was washed in chloroform/acetone (2:2) and dried under vacuum to obtain PGA–PTX conjugate. The supernatant of the chloroform/acetone washing mixture was kept to determine drug loading by measuring the amount of unreacted PTX by analytical HPLC.

2.4.2. Synthesis of SH–PGA–PTX

Cysteamine (12.7 mg, $1.65 * 10^{-1}$ mmol) was bound to the PGA–PTX by carbodiimide coupling in anhydrous DMF (15 ml), in the presence of 50 mM dithiothreitol (DTT) as reducing agent. After 24 hours the solvent was evaporated under high vacuum and the residue dissolved in MilliQ water. This aqueous solution was purified using Sephacryl S-200 HR column to remove unreacted cysteamine. The appropriate fractions were lyophilized to obtain SH–PGA–PTX (elution fractions 85–160 ml). Presence of thiol groups on the polymer was confirmed by Ellman's test [36].

2.4.3. Synthesis of PGA–PTX–DOX

DOX-3,3′-*N*-[ε-maleimidocaproic acid] hydrazide (EMCH) was coupled with SH–PGA–PTX, by selective reaction of the maleimide moiety of the linker with SH groups on PGA, to form the final conjugate PGA–PTX–DOX. Reaction was done in dry DMF (10 ml) with the addition of *tris*(2-carboxyethyl)phosphine (TCEP) as a reducing agent. The water-soluble sodium salt of the conjugate was obtained by dissolving the product in 0.25 M $NaHCO_3$ after evaporation of DMF. This aqueous solution was purified using Sephacryl S-200 HR column, removing unreacted drugs and low molecular weight contaminants, and lyophilized to obtain the final product as a red powder (elution fractions 85–160 ml). DOX loading was determined by measuring the absorbance of the conjugate ($\lambda_{EX} = 495$ nm) and by using the molar absorbance of DOX–EMCH ($\varepsilon = 9250\ M^{-1}\ cm^{-1}$). The conjugate was synthesized in 100 mg scale. Appropriate controls were synthesized (i.e., PGA–PTX (300 mg scale), PGA–DOX (50 mg scale)).

2.4.4. Synthesis of DOX–EMCH

DOX (100.7 mg, $1.74 * 10^{-1}$ mmol) was coupled to an acid-sensitive, EMCH (118.0 mg, $3.48 * 10^{-1}$ mmol) linker in a procedure developed by Willner et al. [37]. MS (ES^+): *m/z*: 752.3 [M], 775.5 $[M + Na]^+$.

2.5. Physico-chemical characterization of the conjugates

2.5.1. Nuclear magnetic resonance (NMR) measurements

^1H NMR was performed on 400 MHz Avance, Bruker (Karlshruhe, Germany) system with tetramethylsilane (TMS) as an internal standard. The spectra were recorded at room temperature (RT) in deuterium oxide (D_2O), except for PTX, which was recorded in deuterated chloroform ($CDCl_3$).

2.5.2. Surface charge measurements of the conjugates

Zeta potential measurements were performed on a Zetasizer Nano ZS analyzer with an integrated 4 mW He–Ne laser ($\lambda = 532$ nm; Malvern Instruments Ltd., Malvern, Worcestershire, U.K.). To elucidate the surface charge of the conjugates, PGA–PTX, PGA–DOX and PGA–PTX–DOX potentials were measured in 20% aqueous phosphate buffered

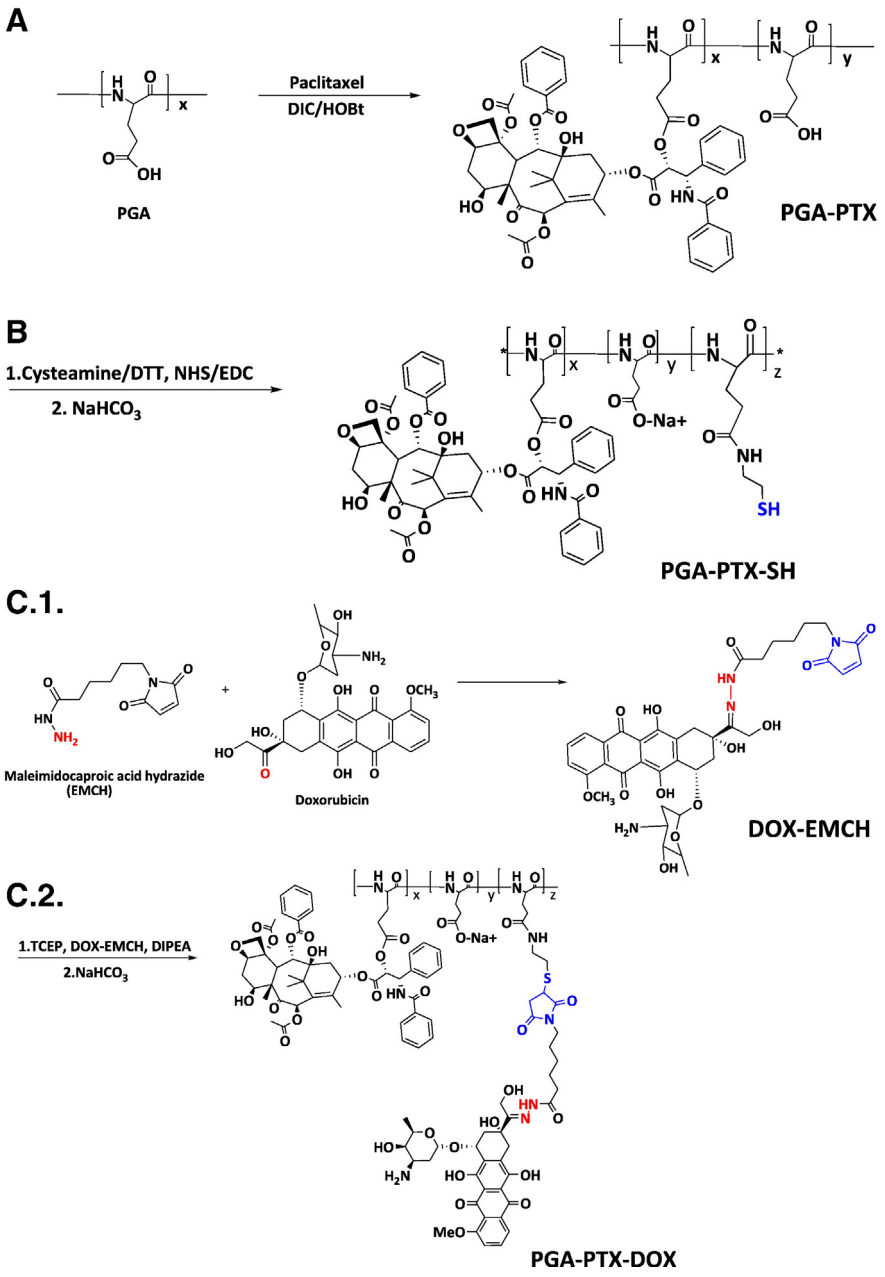

Scheme 1. Synthesis of PGA–PTX–DOX conjugate. **x**: loading of PTX, 2 mol%, **z**: loading of DOX, 5 mol%.

saline (PBS), pH = 7.4. The samples were freshly prepared at a concentration of 0.1 mg/ml, and filtered through 0.2 μm filter. All measurements were performed at 25 °C using folded capillary cells (DTS 1070).

2.5.3. Hydrodynamic diameter measurements of the conjugates

Hydrodynamic diameter was measured by dynamic light scattering (DLS) on a Zetasizer Nano ZS analyzer with an integrated 4 mW He–Ne laser (λ = 633 nm; Malvern Instruments Ltd., Malvern, Worcestershire, U.K.). The samples were freshly prepared in PBS at a concentration of 0.5 mg/ml. All measurements were performed at 25 °C, using polystyrene cuvettes (10 × 4 × 45 mm).

2.6. Drug release profile and polymer degradation kinetics

2.6.1. Paclitaxel release

For cathepsin B-mediated release measurement, conjugates were dissolved at a concentration of 5 mg/ml in freshly prepared activity phosphate buffer pH = 6.0 containing 50 mM NaCl, 1 mM ethylenediaminetetraacetic acid (EDTA) and 5 mM glutathione (GSH), and 0.5 unit/1 ml bovine spleen cathepsin B enzyme (Sigma) was added. For esterase-mediated release, conjugates were dissolved at a concentration of 5 mg/ml in PBS and 10 μl porcine liver esterase solution, 150 μ/mg protein (Sigma) was added to 0.5 ml sample. Samples were incubated at 37 °C. Fifty microliters of aliquots taken each day up to 8 days and 150 μl methanol was added to each sample to extract the drug. Samples were stored at −20 °C in darkness until analysis. The amount of released drug was assayed by HPLC against a calibration curve of free PTX. For non-enzymatic hydrolytic cleavage assessment, polymers were incubated in activity buffer or in PBS only.

2.6.2. Doxorubicin release

Conjugates were dissolved at a concentration of 5 mg/ml in PBS at pH = 5.0 or in PBS at pH = 7.4 and placed in dialysis tubes in 100 ml of the same buffer. Samples (1 ml) were taken each day and the same amount of buffer was replaced. The amount of released DOX was measured by fluorescence (λ_{Ex} = 485 nm). Alternatively, conjugates were

dissolved at a concentration of 5 mg/ml in freshly prepared PBS pH = 5.0, 6.0 or 7.0. Samples (100 μl) were taken every day and injected to HPLC equipped with SEC column.

2.7. Cell culture

MDA-MB-231 human breast cancer cells and ES-2 human ovarian carcinoma cells were obtained from the American Type Culture Collection (ATCC). Both cancer cell lines, MDA-MB-231 and ES-2, were grown in Dulbecco's modified Eagle's medium (DMEM) supplemented with 10% fetal bovine serum (FBS), 100 mg/ml Penicillin, 100 U/ml Streptomycin, 12.5 U/ml Nystatin (PSN), and 2 mM L-glutamine (L-Glu). Cells were grown at 37 °C; 5% CO_2.

2.7.1. Cell proliferation assay

Cells were plated onto 24-well plates (1×10^4 cells/well for both cell lines) and allowed to attach for 24 hours. Cells were incubated with the conjugates and free drugs, dissolved in cell culture medium at serial concentrations, for 72 hours. For treatments containing PTX concentrations ranged from 0.01 nM to 1000 nM, according to PTX-equivalent concentration. For DOX and PGA–DOX concentrations ranged from 0.025 nM to 2500 nM, according to DOX-equivalent concentration. These concentrations were selected in order to have the same molar ratio of PTX to DOX in all the controls as in the PGA–PTX–DOX conjugate (1:2.5 PTX/DOX, respectively). PGA was used at concentrations equivalent to PGA content in PGA–PTX–DOX conjugate. Following incubation, cells were washed, detached by trypsin and counted by Coulter Counter® (Beckman Coulter).

2.7.2. Isobolograms of PTX and DOX drug combination treatments

IC_{50} represents the concentration of a drug that is required for 50% inhibition *in vitro*. The $IC_{30,\ 50,\ 70}$ values of treatment with PTX, DOX and their combinations were calculated from the proliferation assays. $IC_{30,\ 50,\ 70}$ values of PTX and DOX were marked on *X*, *Y* axes respectively and a line which represents additive effect was drawn between each inhibitory concentration (IC). The combination index (CI) of each treatment was calculated according to the classic isobologram equation combination index = $[(D)1/(Dx)1] + [(D)2/(Dx)2]$ as previously described [38]. Area on the right side of each IC additive line represents antagonistic effect and the left side represents synergistic effect.

2.7.3. Migration (scratch) assay

The migration of ES-2 and MDA-MB-231 cells in the presence of PGA–PTX–DOX conjugate and controls was evaluated using the scratch assay. A scratch was done on a confluent cell monolayer, and cells were incubated with the conjugates and the free drugs at PTX-equivalent concentrations of 100 nM and DOX-equivalent concentrations of 250 nM for 17 hours for ES-2 cells and 24 hours for MDA-MB-231 cells. Plates were imaged and the gap width was measured in the beginning and end of the experiment, at the same reference point.

2.7.4. Intracellular uptake of PGA–PTX–DOX conjugate by confocal microscopy

MDA-MB-231 cells were seeded on cover glasses placed in 24-well plates and allowed to attach for 24 hours. Cells were incubated with PGA–DOX, PGA–PTX–DOX or free DOX (DOX-equivalent concentration of 500 nM) for 0.5, 4, 12, 24 or 36 hours, washed with PBS, fixed with 4% paraformaldehyde (PFA) for 20 minutes at RT and washed with PBS again. Slides were mounted with Prolong Gold® antifade reagent with 4′,6-diamidino-2-phenylindole (DAPI) (Invitrogen). Cellular uptake was imaged with a Leica SP5 Confocal Imaging system.

2.8. Biocompatibility evaluation

2.8.1. Cytokines induction assay

We evaluated the effect of conjugates (PGA–PTX–DOX, PGA–PTX, PGA–DOX, PGA–PTX plus PGA–DOX), free drugs (PTX, DOX and PTX plus DOX) and PGA alone on tumor necrosis factor alpha (TNF-α) and interleukin 6 (IL-6) cytokines secretion from human peripheral blood mononuclear cells (PBMCs). PBMCs were freshly isolated from healthy human donors obtained from Tel Hashomer (Sheba) Blood Bank. Whole blood was diluted with PBS in a ratio of 1:2. The diluted blood was gently overlaid onto 10 ml Ficoll (lymphoprep) (1:3 ratio). Gradients were centrifuged at 22 °C, 300*g* (1400 rpm), for 30 minutes. Opaque-light PBMCs ring was removed from the interphase into a new tube. PBMCs were washed with PBS and centrifuged at 250*g* (1100 rpm) for 10 minutes. PBMCs pellet was resuspended in approximately 40 ml Roswell Park Memorial Institute (RPMI) 1640 growth medium (with 10% FBS, L-Glu, PSN). Cells were resuspended with PBMCs medium to a final concentration of 8×10^6/ml. PBMCs (1 ml/sample) were incubated with the conjugates or free drugs for 4 hours at 37 °C in humidified 5% CO_2/air. Lipopolysacharides (LPS) (L2880, Sigma) were used as positive control (1 mg/ml) and PBS was used as negative control. Upon incubation, cells were centrifuged at 200*g* (1000 rpm) for 5 minutes. Supernatant was removed and RNA was isolated from the cells pellets using EZ-RNA II total RNA isolation kit (Biological Industries). One microgram of RNA was reverse transcribed using EZ-first strand cDNA synthesis kit for RT-PCR (Biological Industries). SYBR green based real-time PCR assays (QIAGEN) were used to assess the levels of TNF-α and IL-6 cytokines secretion following incubation of PBMCs with the tested conjugates. The expression levels of the evaluated cytokines were normalized to GAPDH. The following primer pairs were used: IL-6: F—GGCACTGGCAGAAAACAACC, R—GGC AAGTCTCCTC AT TGA ATCC; TNF-α: F—CCCAGGCAGTCAGATCATCTTC, R—TCAGCT TGAGGGTTTGCTACAA; GAPDH: F—ATTCCACCCATGGCAAATTC, R—GGATCTCGCTCC TGGAAGATG.

2.8.2. Hemolysis assay

Rat red blood cells (RBC) solution (2% wt/wt) was incubated with serial dilutions of PGA–PTX–DOX, PTX, DOX and the combination of free drugs, for 1 hour at 37 °C. Highest concentration of the treatments was the one used in the *in vivo* experiment, adjusted to dilution in mouse blood volume (0.5 mg/ml conjugate and equivalent concentrations of free drugs). Dextran (Mw 70 kDa, Sigma) was used as negative control and polyethyleneimine (Mw 25 kDa, Sigma) was used as positive control. Following centrifugation, the supernatants were transferred to a new plate and absorbance measured at 550 nm using a SpectraMax M5^e plate reader (Molecular Devices). The results were expressed as percentage of hemoglobin released by 1% wt/vol solution of Triton X100 (100% lysis).

2.9. Biodistribution of the conjugate

PGA–PTX–DOX was injected intravenously (i.v.) via the tail vein to nu/nu mice bearing mammary tumors ($n = 3$). Mice were killed following 1.5, 5.5 or 24 hours, perfused with saline and organs and tumors were taken for analysis. Organs and tumor were homogenized and lyophilized. ACN (1 ml) was added to extract the free drugs, and suspension was vortexed well and centrifuged. Supernatant (0.5 ml) was dried by SpeedVac and the obtained residue was dissolved in 100 μl ACN, to concentrate the solution. To the remaining organs suspension 1 ml DDW was added, to extract the water-soluble conjugate. Same procedure as for ACN was repeated. The resulting 100 μl solutions were injected to HPLC to determine the amount of the conjugate and the released drugs.

2.10. Evaluation of antitumor activity and toxicity of the conjugates

Nu/nu female mice were inoculated to the mammary fat pad with 1×10^6 MDA-MB-231 cells. Mice bearing ~25 mm^3 tumors were treated i.v. with conjugates (PGA–PTX–DOX ($n = 3$), PGA–PTX ($n = 4$), PGA–DOX ($n = 4$) and combination of PGA–PTX and PGA–DOX in the same ratio as on the PGA–PTX–DOX conjugate ($n = 4$)), free drugs (PTX ($n = 4$), DOX ($n = 4$) and PTX + DOX combination in the same ratio as on the PGA–PTX–DOX conjugate ($n = 5$)) and PBS + 20 mM DTT ($n = 3$). All drugs and conjugates solutions were prepared with PBS containing 20 mM DTT as a reducing agent, to prevent aggregate formation in the conjugate solutions. First treatment was given at 7.5 mg/kg DOX-equivalent dose and 4.5 mg/kg PTX-equivalent dose, and the following treatments at 5 mg/kg DOX-equivalent dose and 3 mg/kg PTX-equivalent dose. Mice were treated three times a week, starting at day 11 post-tumor inoculation (5 treatments in total). Tumors were measured by a digital caliper and tumor volume was calculated as: $width^2 \times length \times 0.52$. Body weight and tumor size were monitored every other day. Mice were sacrificed when tumor volume reached 1500 mm^3 or when they lost more than 15% of their body weight.

2.11. Statistical methods

Data were expressed as mean ± SD for *in vitro* assays or ± SEM for *in vivo*. Statistical significance was determined using an analysis of variance (ANOVA).

3. Results

3.1. Physico-chemical characterization of the conjugates

A PGA-based conjugate bearing PTX and DOX (PGA–PTX–DOX) and control conjugates (PGA–PTX and PGA–DOX) have been synthesized and characterized. Synthesis of the PGA–PTX–DOX conjugate is depicted in Scheme 1. ^1H NMR (400 MHz, D_2O) confirmed the coupling of PTX and DOX to PGA (Supplementary Fig. 1). SEC analysis of PGA–PTX–DOX showed a peak with retention time of 6.4 minutes, corresponding to high Mw compounds, and absorbance at 270 nm and 485 nm indicating the presence of PTX and DOX, respectively, on the polymer (Supplementary Fig. 2).

3.1.1. Drug loading of the conjugates

PTX loading was determined indirectly by HPLC, by determining the unbound drug amount. DOX loading was determined by UV, using the molar absorbance coefficient of DOX–EMCH. For PGA–PTX–DOX conjugate, PTX loading was 2 mol% (8.3% wt/wt) and DOX loading was 5 mol% (13.2% wt/wt). For PGA–PTX conjugate, loading was 13.5 mol% (44.0% wt/wt) and for PGA–DOX conjugate, loading was 2.8 mol% (8.8% wt/wt).

3.1.2. Zeta potential of the conjugates

Zeta potential of PGA and the conjugates was measured. Zeta potential values are summarized in Table 1. As expected, PGA was negatively charged, and it became less negative when the drugs were bound to the $^{\gamma}$COOH residues.

3.1.3. Hydrodynamic diameter of the conjugates

Hydrodynamic diameter of the conjugates was measured. The values are summarized in Table 1. PGA–PTX–DOX has the largest diameter (37.5 nm), compared with PGA–PTX and PGA–DOX, as expected for a polymer bearing two drugs. PGA–DOX was found to have a larger diameter compared to PGA–PTX (17.0 nm versus 4.6 nm, respectively). PGA was found to be of 4.5 nm.

The physicochemical parameters of the conjugates are summarized in Table 1.

3.1.4. Release of the drugs

Release of the drugs from the conjugates was evaluated in different conditions (Fig. 1). PTX release was determined in PBS at pH = 6.0 or 7.0 in the presence or absence of cathepsin B or esterase. Release rate was similar at pH = 6.0 or 7.0 and was slightly higher in the presence of cathepsin B or esterase. In any case, only a limited percentage (up to 25%) of the bound PTX was released by the last time point (t = 6 days). Similar release profile was observed for PGA–PTX, even though it has higher loading of PTX (13.5 mol% compared to 2 mol%) (Supplementary Fig. 3). Release of PTX could not be followed for a longer period because degradation of free PTX occurred when incubated longer than 1 week in all the conditions examined (results not shown).

Release of DOX in solution could not be seen in these experiments. When injected to HPLC with SEC column, peak of the conjugate retained the same absorbance at the 485 nm wavelength at all the time points (up to 7 days).

3.1.5. Stability evaluation

Drug release in PBS at 37 °C from PGA–PTX–DOX was 8% and from PGA–PTX, it was 5% after 24 hours.

3.2. Cell culture experiments

3.2.1. Evaluation of synergistic activity of drug combination

Effect of combination treatment of PTX and DOX was evaluated on several cancer cell lines at different ratios of the drugs. Combination of the drugs showed synergism on MDA-MB-231 and ES-2 cells, which was highest when DOX was in higher concentration than PTX (Fig. 2). Combination index (CI) of these drugs was evaluated in several other cell lines and was found to be cell line-dependent (results not shown).

3.2.2. Evaluation of the cytotoxic effect of PGA–PTX–DOX conjugate on cancer cells

Cytotoxicity of free drugs, PGA–PTX–DOX conjugate, PGA–PTX and PGA–DOX conjugates was evaluated on ES-2 ovarian carcinoma cells and MDA-MB-231 breast cancer cells. PGA–PTX–DOX exhibited high cytotoxicity, as did a combination of PGA–PTX and PGA–DOX (Fig. 3). Free drugs were more toxic than the conjugates. PGA alone exhibited no toxicity up to the concentrations relevant for the *in vivo* study. IC_{50} values of the treatments are summarized in Table 2. Results are an average of three independent experiments.

3.2.3. Evaluation of the effect of PGA–PTX–DOX conjugate on migration of cancer cells

The migration of ES-2 cells and MDA-MB-231 cells in the presence of PGA–PTX–DOX conjugate was evaluated using the scratch assay. PGA–PTX–DOX significantly inhibited the migration of the cells compared

Table 1
Physico-chemical properties of the conjugates.

	Size (d, nm)	Zeta potential (mV)	Molecular weight (theoretical) (kDa)	PTX loading (%mol)	DOX loading (%mol)
PGA salt form	4.5	−42.5	15.1	–	–
PGA–PTX–DOX	37.5	−27.3	20.7	2.0	5.0
PGA–PTX	4.6	−30.4	26.1	13.5	–
PGA–DOX	17.0	−35.9	17.3	–	2.8

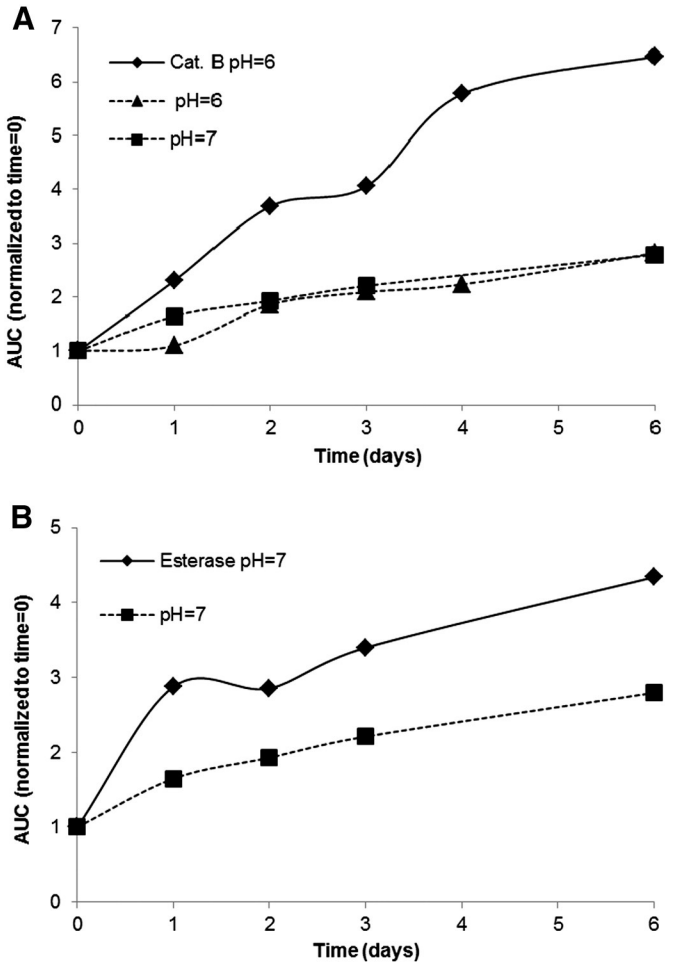

Fig. 1. PTX release from the polymer. (A) Release of PTX in the presence of cathepsin B at pH 6, at 37 °C. (B) Release of PTX in the presence of esterase in PBS, at 37 °C.

to all other controls (Fig. 4). Representative results from one of three independent experiments are shown.

3.2.4. Intracellular uptake of PGA–PTX–DOX conjugate

Internalization and accumulation of DOX in the nucleus of ES-2 cells and MDA-MB-231 cells was evaluated by confocal microscopy. In all samples, DOX was seen inside the cells already at the 30 minutes time point, indicating rapid internalization both for free drug and the conjugates. Free DOX is seen in the nucleus of the cells after 4 hours. In the PGA–DOX samples, DOX is seen in the nucleus after 12 hours, while in the PGA–PTX–DOX samples, DOX is accumulated in the nucleus by 36 hours for both cell lines (Fig. 5A, B). A spectral analysis of the images revealed a shift in the spectrum of DOX when it is inside the nucleus, indicating that DOX is not bound to the polymer when in the nucleus (Supplementary Fig. 4).

3.3. Biocompatibility evaluation

3.3.1. Cytokines induction

In order to evaluate the safety profile of PGA–PTX–DOX as a nanomedicine, an *ex vivo* cytokines induction study was performed using the human PBMCs, which determined the secretion of major inflammatory cytokines. The secretion level of inflammatory interleukins was evaluated using IL-6 and TNF-α as a model for the innate immune response. PGA–PTX–DOX did not induce elevated secretion of the cytokines, while free DOX did. As a positive control, we used the Toll-like receptor 4 natural ligand, lipopolysaccharides (LPS), that induced secretion of high levels of both TNF-α and IL-6 (Fig. 6).

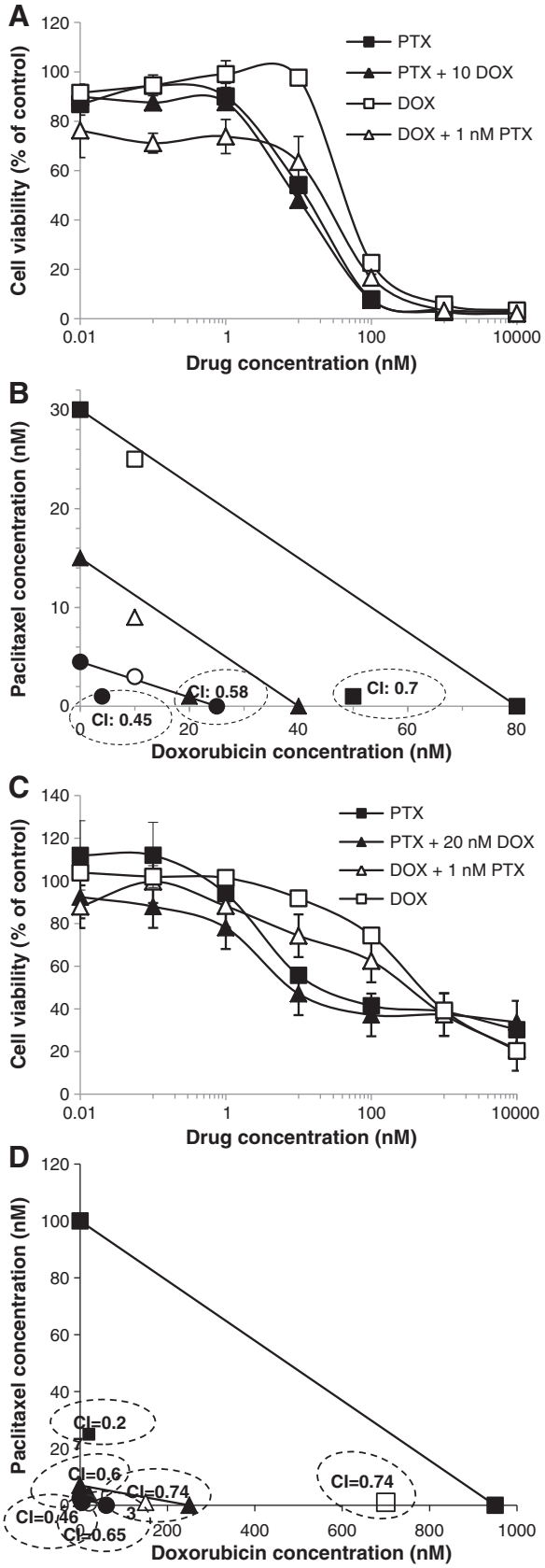

Fig. 2. Synergistic activity of PTX and DOX on cancer cells. Inhibition of cell proliferation and isobolograms of drug combination on (A, B) ES2 and (C, D) MDA-MB-231 cells. The IC values were calculated from the logarithmic trendlines of the curves (see Supplementary Table 1 for trendline equations).

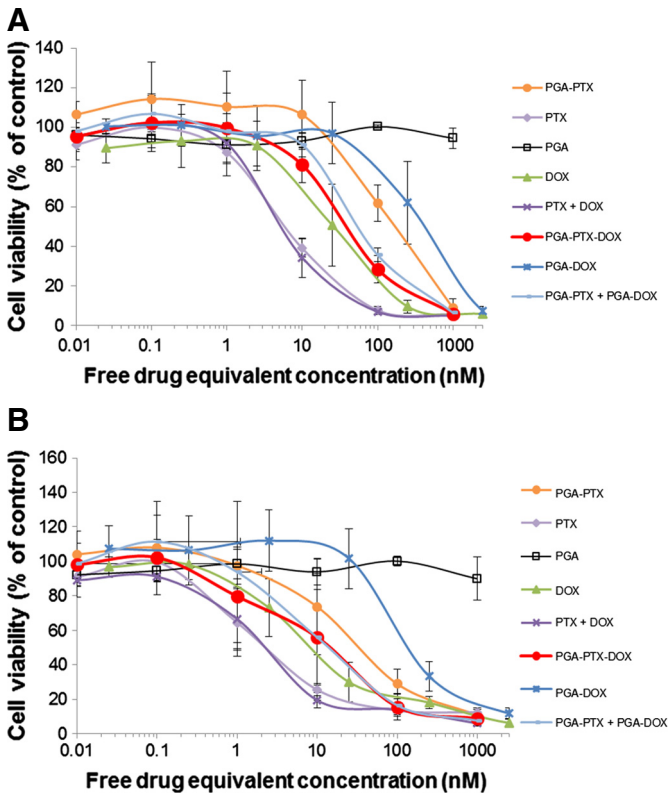

Fig. 3. Growth inhibition of cancer cells by PGA–PTX–DOX conjugate. Drugs retain their cytotoxic effect after conjugation to the polymer. Cells were incubated with the conjugates and free drugs, dissolved in cell culture medium at serial concentrations, for 72 hours. PGA–PTX–DOX conjugate inhibited the growth of (A) ES2 cells and (B) MDA-MB-231 cells, similarly to the combination of PGA–PTX + PGA–DOX, but less than the combination of free drugs. PGA had no cytotoxic effect.

3.3.2. Hemolysis

Biocompatibility of the conjugate was also assessed by measuring red blood cell (RBC) lysis. The concentrations used were the relevant *in vivo* concentrations, adjusted to dilution in the mouse blood volume (1.5 ml). The results clearly show that at this concentration our PGA–PTX–DOX conjugate and the free drugs did not cause hemolysis *ex vivo* and are therefore suitable for i.v. administration (Fig. 7). Polyethyleneimine (PEI), a cationic polymer, was used as a positive control and dextran was used as a negative control.

3.4. Biodistribution of the conjugate

Biodistribution of the PGA–PTX–DOX conjugate in mammary adenocarcinoma-bearing mice was evaluated following i.v. administration. Amounts of conjugate in organs and tumors were evaluated by analytical RP-HPLC, using a calibration curve of PGA–PTX–DOX conjugate. The conjugate accumulated mainly in the tumor (Fig. 8). Some amount of the conjugate was also detected in the kidneys and in the spleen.

Table 2
IC_{50} values (nM) of the conjugates and free drugs.

Treatment/Cells	ES-2	MDA-MB-231
PTX	5	4
DOX	22	16
PTX + DOX	6	2
PGA–PTX–DOX	29	10
PGA–PTX	233	31
PGA–DOX	211	190
PGA–PTX + PGA–DOX	47	13
PGA	NA	NA

NA–not applicable. The IC_{50} values were calculated from the logarithmic trendlines of the curves (see Supplementary Table 2 for trendline equations).

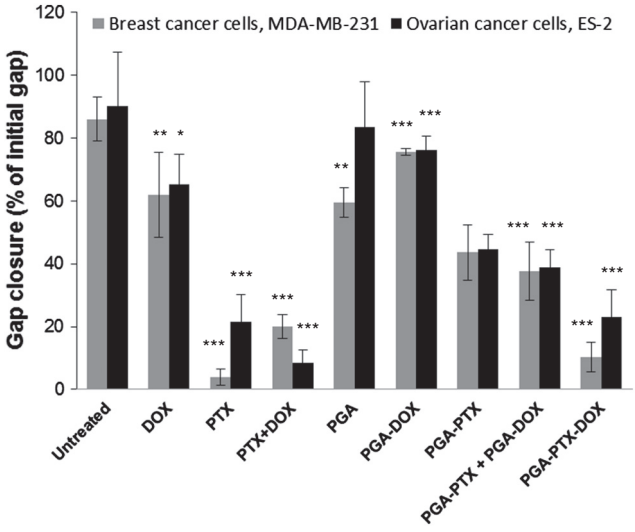

Fig. 4. Inhibition of cancer cell migration (scratch assay) by PGA–PTX–DOX conjugate. PGA–PTX–DOX inhibited the migration of ES2 (black) and MDA-MB-231 (gray) cells similarly to free PTX and combination of free drugs (PTX + DOX). Statistical significance was determined using one-sided ANOVA and Dunnett post hoc test. $^{*}p < 0.05$, $^{**}p < 0.01$, $^{***}p < 0.001$, compared to untreated control.

3.5. Evaluation of antitumor activity and toxicity of the conjugates

3.5.1. Efficacy

Treatment with PGA–PTX–DOX conjugate led to a substantial antitumor effect in human mammary adenocarcinoma mouse model, compared with controls. Notably, the PGA–PTX–DOX conjugate inhibited tumor growth to a higher extent than the mixture of individually-conjugated drugs (PGA–PTX + PGA–DOX) or the combination of free drugs (PTX + DOX) at equivalent drug-concentrations (Fig. 9A). The graph of each group was terminated on the day at which the initial number of the mice was reduced due to toxicity or tumor size. However, measurements of remaining mice in the group continued and are shown in the Kaplan–Meyer survival curve. Treatment efficacy, defined as tumor growth inhibition ratio between treated versus control groups (T/C), was calculated on day 26 following treatment initiation, when first mouse was euthanized due to large tumor size (Table 3). Mice treated with PGA–PTX–DOX conjugate survived for the longest period of all groups (Fig. 9B).

3.5.2. Safety

The conjugates exhibited superior safety compared to the free drugs. Five treatments with free DOX (5 mg/kg) and combination of PTX plus DOX (3 + 5 mg/kg, respectively) caused a reduction of over 10% in body weight immediately following treatments, which was reversed after treatment withdrawal. Several weeks later, mice from these groups developed again significant weight loss and appeared weak and lethargic. Mice that lost more than 15% body weight were euthanized (3 out of 5 mice in each of these groups). Mice treated with conjugates, PBS or free PTX (5 treatments of 3 mg/kg) exhibited stable weight gain and appeared healthy (Fig. 9C). Furthermore, mice from the DOX- and PTX plus DOX-treated groups also developed tail skin lesions at the site of injection about a week following treatment withdrawal (Fig. 9D).

4. Discussion

The aims of this study were to synthesize a novel polymer therapeutic combining two synergistic drugs on the same polymer chain at an appropriate ratio, and to determine its advantage over drugs conjugated to separate polymer chains and over the combination of free drugs. PTX and DOX were selected because they are highly potent anticancer agents, which are used extensively in the clinic as mono-therapies and

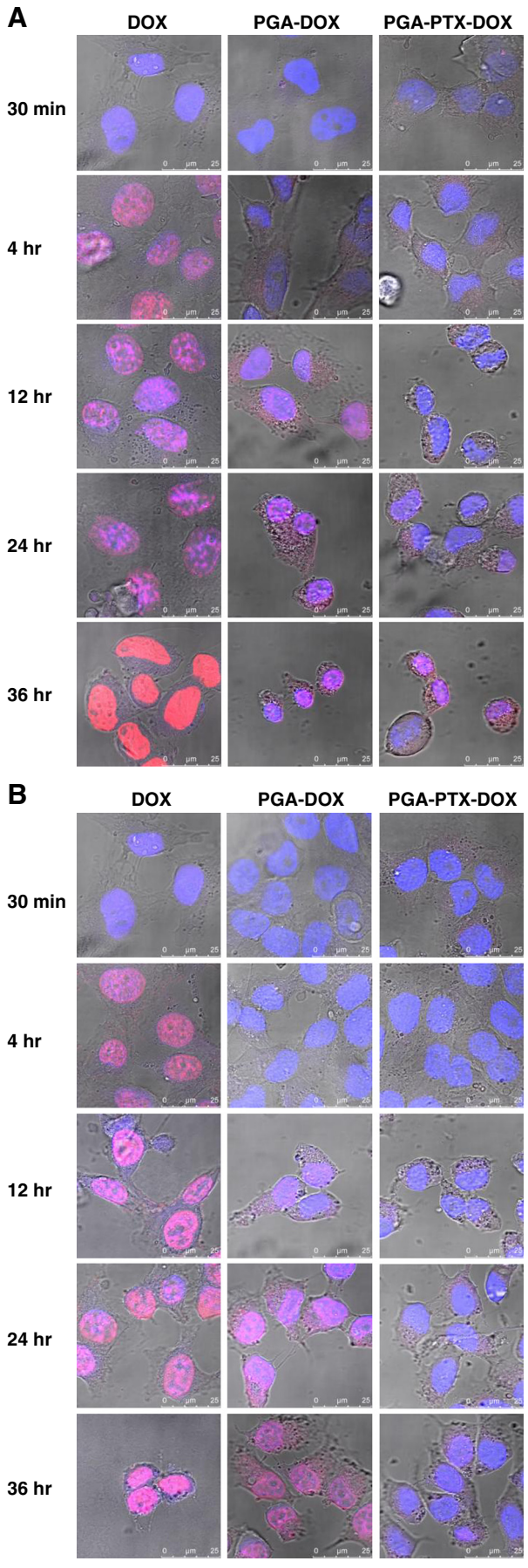

in sequential combination protocol, especially for the treatment of metastatic breast cancer [16,17]. Our system demonstrates for the first time a covalent bonding of PTX and DOX to the same polymeric backbone, PGA. Several studies suggested a combination of two drugs using a single polymeric backbone as a carrier. Some of these studies evaluated the *in vitro* activity of DOX in combination with other agents. Vicent et al. [31] showed an *in vitro* synergistic effect with a synthetic polymer carrying a chemotherapeutic agent (DOX) and an endocrine therapy (aminoglutethimide, AGM) designed for the treatment of postmenopausal breast cancer patients. Furthermore, Greco et al. [39] compared the cytotoxic activity of HPMA copolymer–DOX–AGM conjugate to the combination of each drug bound separately to HPMA copolymer. They showed that attachment of both drugs to the same polymer backbone was a requirement for enhanced cytotoxicity, and that a mixture of polymer conjugates containing only AGM and only DOX did not show synergistic benefit *in vitro* [31,39]. Bae et al. [40] evaluated a PEG–poly(aspartate-hydrazide) (PEG–PAH) block copolymer of DOX for combination delivery with Wortmannin (WOR), a phosphatidylinositol-3 kinase inhibitor. pH-sensitive polymeric micelles were designed to release the two agents simultaneously with an identical pharmacokinetic profile. *In vitro* biological activity revealed that by concurrent treatment of DOX and WOR, enhanced cytotoxicity was observed. Unfortunately, WOR is not an FDA-approved drug. In addition to these promising *in vitro* findings showing advantageous DOX combinations, *in vivo* evidence for the potential of polymer-based multi-drug targeting was provided by Ahmed et al. [41], that showed *in vivo* anticancer activity of biodegradable polymersomes loaded with a combination of PTX and DOX. In their study, the microphase transitions of the polymersomes fostered the drug release, first of the soluble DOX and then of PTX, that was integrated into the membrane. The release of the drugs occurred at neutral pH. However, unlike our covalently-conjugated PTX and DOX, these drugs were entrapped in the polymersomes [41]. A recent study by Lammers et al [32]. presented a modest therapeutic benefit *in vivo* of HPMA copolymer conjugated to DOX and gemcitabine (Gem), over the combination of the two individual polymeric prodrugs. The authors speculated that this modest effect might be attributed to the cell lines' low sensitivity to DOX [32]. For all above mentioned studies, a synergistic effect with DOX was not fully demonstrated by isobolograms and combination indexes, thus it is difficult to compare between the studies.

Another example of combination therapy involving PTX is a codelivery of PTX and cisplatin (CDDP) loaded on a triblock polypeptide, forming a micellar carrier. The dual-drug-loaded micelles showed synergistic effects in inhibition of proliferation of human lung cancer cells. Similarly to our results, an *in vivo* study showed that the polypeptide-based combination of the two drugs displayed safer and more efficacious inhibition toward tumor growth than free drug combination [34].

Before coupling PTX and DOX to the carrier, we thoroughly investigated the optimal ratio of drugs for synergism and the different types of cancer cells in which synergism occurs. Our results show that these drugs have a synergistic cytotoxic activity on MDA-MB-231 breast cancer cells and ES-2 ovarian cancer cells, when DOX is at higher concentration than PTX, according to calculated isobolograms. Our final conjugate had a loading of 5 mol% DOX and 2 mol% PTX that resulted in drug synergism. Due to synthetic limitations, a higher loading of DOX could not be achieved. A higher PTX loading was easily achieved as demonstrated for PGA–PTX at 13.5 mol%. However, it was necessary to limit the PTX loading in order to obtain a synergistic ratio of DOX to PTX on the polymer. The zeta potential of the polymer remained

Fig. 5. Internalization of PGA–PTX–DOX conjugate into cancer cells. Internalization of PGA–PTX–DOX conjugate, PGA–DOX conjugate and free DOX into (A) ES2 and (B) MDA-MB-231 cells was examined by confocal microscopy after incubation with the drug for 0.5, 4, 12, 24 and 36 hours. After 30 minutes both the conjugate and free DOX were seen inside the cells, indicated by red color of the DOX. Free DOX was concentrated in the nucleus after 4 hours, while in PGA–DOX samples DOX was observed the nucleus after 12 hours and in PGA–PTX–DOX samples after 24 hours.

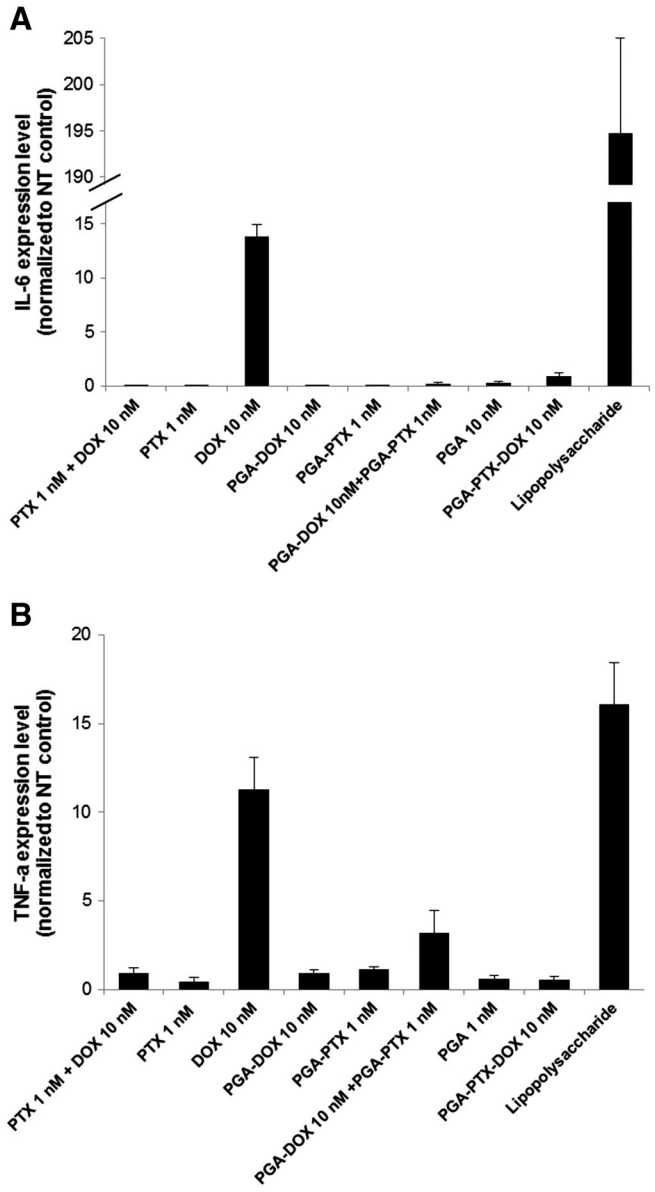

Fig. 6. PGA–PTX–DOX does not induce cytokine release from PBMCs. Release of pro-inflammatory cytokines (A) IL-6 and (B) TNF-alpha from human PBMCs after 4-hour incubation with PGA–PTX–DOX conjugate and the control treatments. PGA–PTX–DOX did not induce release of the cytokines, while free DOX did. LPS was used as a positive control.

negative after conjugation of the drugs, which should confer good formulation stability by reducing aggregation.

In principle, both drugs should have similar release kinetics from the polymer in order to achieve synergism at the target site. In our nano-sized conjugate, DOX was bound through an acid-labile hydrazone linker, which is cleaved in acidic pH such as that of the endosome or lysosome. PTX was bound directly to the PGA backbone via an ester bond that can be hydrolyzed in the same cellular compartments as the EMCH linker, in acidic pH and by esterases. Our results show that in the presence of esterase or cathepsin B, release of PTX from the polymer was slightly faster than in PBS. Degradation of the polymer chain by cathepsin B enhances the release of PTX. Since the linker between the PGA and PTX is a hydrolytically-labile ester bond, our initial concern was whether premature release of PTX in the circulation would undermine the conjugate's ability to reduce systemic toxicity. Previous work on PGA–PTX using a similar linker showed a small PTX fraction being released in the circulation [42]. These findings together with the results obtained from our PTX release experiments (Fig. 1) suggest that PTX

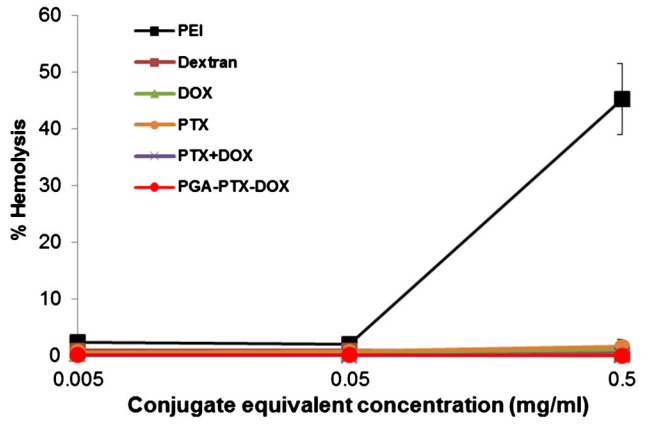

Fig. 7. PGA–PTX–DOX does not cause red blood cell lysis. Hemolysis of RBC isolated from whole rat blood was examined after 1-hour incubation with PGA–PTX–DOX conjugate and the control treatments. None of the treatments caused hemolysis at the concentrations used in *in vivo* experiments. PEI was used as a positive control and dextran as a negative control.

release in the plasma was at a minimal amount and did not induce any toxicity (Fig. 9C and D).

We could not detect the release of DOX from the polymer in solution, even after prolonged incubation at acidic pH. However, we demonstrate that DOX is being released from the polymer intracellularly, as evidenced by confocal microscopy experiments and *in vitro* activity assays. One possible explanation is that the conjugate is forming a complex structure in solution, where the multiple sodium carboxyl groups of the PGA are buffering the external pH, thus preventing the hydrolysis of the acid-labile hydrazone bonds inside. This might also explain the slow release of PTX in solution, while the *in vitro* activity of the conjugates suggests that actual release inside the cells occurs much faster.

Cell internalization and nuclear accumulation of the conjugated DOX were evaluated by confocal microscopy, using its intrinsic fluorescence. Both free DOX and the conjugates internalized into the cells, but not into the nucleus, by 30 minutes. Free DOX accumulated in the nucleus faster than conjugated DOX, since in order to enter the nucleus, the drug first needs to be released from the polymer [43,44]. DOX from the PGA–PTX–DOX conjugate seems to be released slower than from PGA–DOX, as it is seen to accumulate at a later time point. Probably, the presence of the hydrophobic PTX molecules in the conjugate changes its conformation and therefore the release kinetic of DOX.

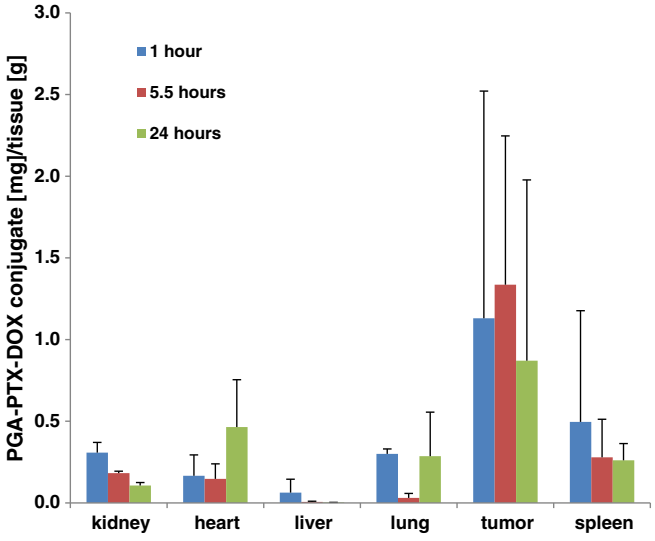

Fig. 8. Biodistribution of PGA–PTX–DOX in mammary tumor bearing mice. Biodistribution of the conjugate at 1.5, 5.5 and 24 hours following i.v. injection. The conjugate accumulated mainly in the tumor at all time points.

In vitro cytotoxicity assays proved that indeed DOX is released in its active form. PGA–PTX–DOX was highly cytotoxic to both MDA-MB-231 and ES-2 cells, suggesting that PTX and DOX are released from the polymer and retain their activity within 72 hours. As expected, *in vitro* free drugs had a higher IC_{50} than conjugated ones, since free drugs enter the cells by diffusion while conjugated drugs first need to be internalized by endocytosis and released from the polymer in order to exert their action [3].

In addition, PGA–PTX–DOX significantly inhibited the migration of MDA-MB-231 and ES-2 cells. This effect is due to the known anti-migratory activity of PTX [21,45–47].

Release of IL-6 and TNF-alpha, two major pro-inflammatory cytokines, from human peripheral blood mononuclear cells was used as a model for innate immune response [48]. None of the conjugates induced the release of the cytokines. Interestingly, free DOX caused release of the cytokines, while a combination of PTX plus DOX did not.

PGA–PTX–DOX conjugate also had no hemolytic activity in an *ex vivo* RBC lysis assay, at the concentrations relevant to the *in vivo* experiment (0.5 mg/ml conjugate, equivalent to 5 mg/kg DOX for 20 g mouse with 1.5 ml blood volume).

Biodistribution analysis of PGA–PTX–DOX demonstrated preferred accumulation of the conjugate in tumors at all time points. The accumulation of the conjugate in the kidneys is most probably due to renal excretion that was already apparent 1.5 hours following injection of the conjugate. Some amount of the conjugate was also detected in the spleen suggesting splenic clearance of particles by the reticuloendothelial system [49] Treatment with PGA–PTX–DOX conjugate led to a substantial antitumor effect on human mammary adenocarcinoma mouse model, compared with controls. We performed a relatively long-term follow-up (151 days), compared to the other studies on polymer–drug conjugates bearing combination therapy. Examining our results in the short-term (26 days) revealed even better results in terms of inhibition of tumor growth (see insert enlarged, Fig. 9A). As expected, the main advantage of the PGA–PTX–DOX conjugate over the combination of PGA–PTX and PGA–DOX was seen *in vivo*. Both treatments exhibited a similar IC_{50} *in vitro*, however, the *in vivo* antitumor activity of the combined PGA–PTX–DOX conjugate was greatly enhanced compared to that of the combination of drugs conjugated to polymers separately. This confirms that there is an advantage to conjugating two drugs to the same polymer chain, as it allows synergism by delivering both drugs to the same target cells simultaneously and at the desired ratio.

It is noteworthy that even though PGA–DOX internalized to breast and ovarian cancer cells and indeed inhibited their proliferation (IC_{50} = 400 nM and 150 nM for ES-2 and MDA-MB-231, respectively),

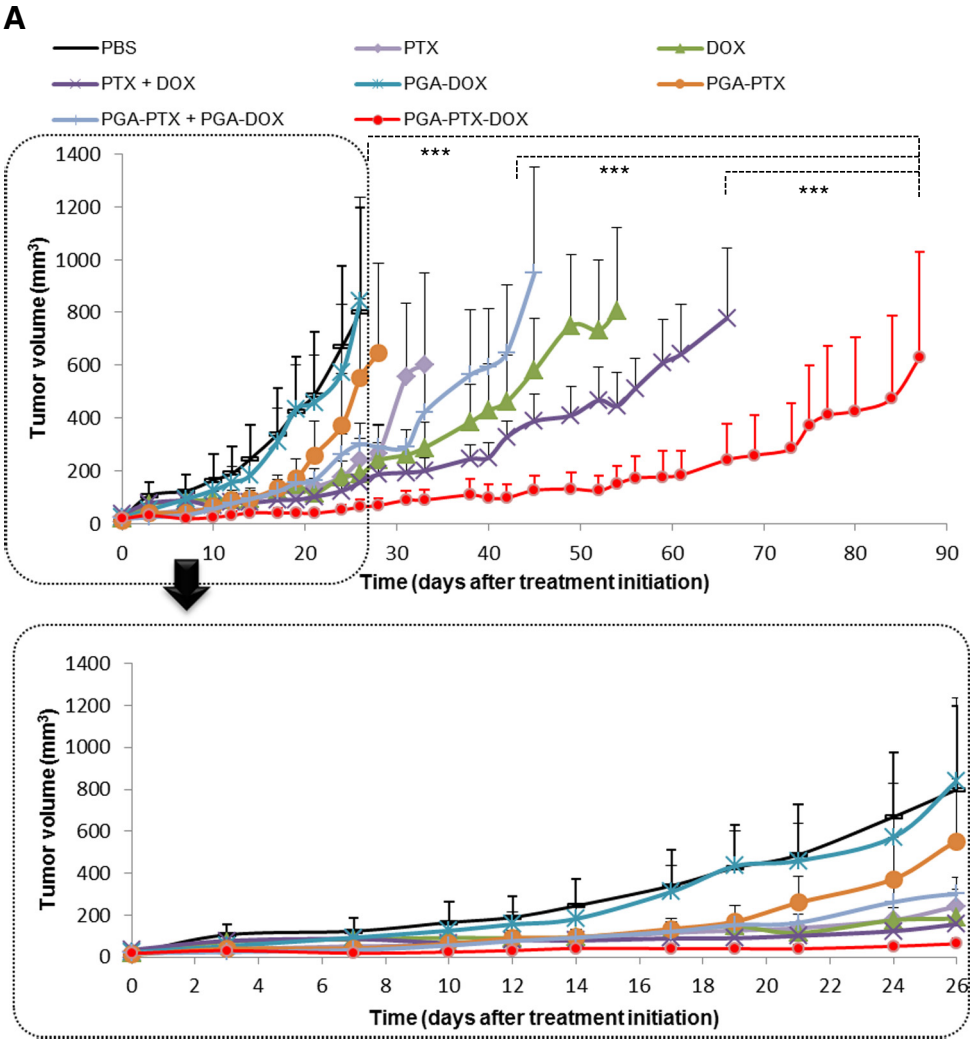

Fig. 9. Antitumor activity and safety of PGA–PTX–DOX in mammary tumor bearing mice. (A) PGA–PTX–DOX conjugate inhibited tumor volume growth more than the combination of PTX and DOX conjugated to separate polymer chains (PGA–PTX + PGA–DOX) and the combination of free drugs (PTX + DOX) in equivalent concentrations. Insert below graph shows close-up of results up to 26 days following treatment initiation. Data represent mean ± SEM. Statistical significance was determined using two-sided repeated-measures ANOVA (***$p < 0.001$). (B) Kaplan–Meyer survival curve. Mice in the PGA–PTX–DOX group had the longest overall survival. (C) Mice treated by free drugs (DOX and PTX plus DOX) suffered from substantial weight loss as opposed to mice treated with conjugates immediately following treatment and also several weeks later. Data represent mean ± SEM. (D) Representative images of tail skin lesions that developed a week after the end of treatments in free drugs groups (lower panel), while mice in conjugate groups had no lesions (upper panel).

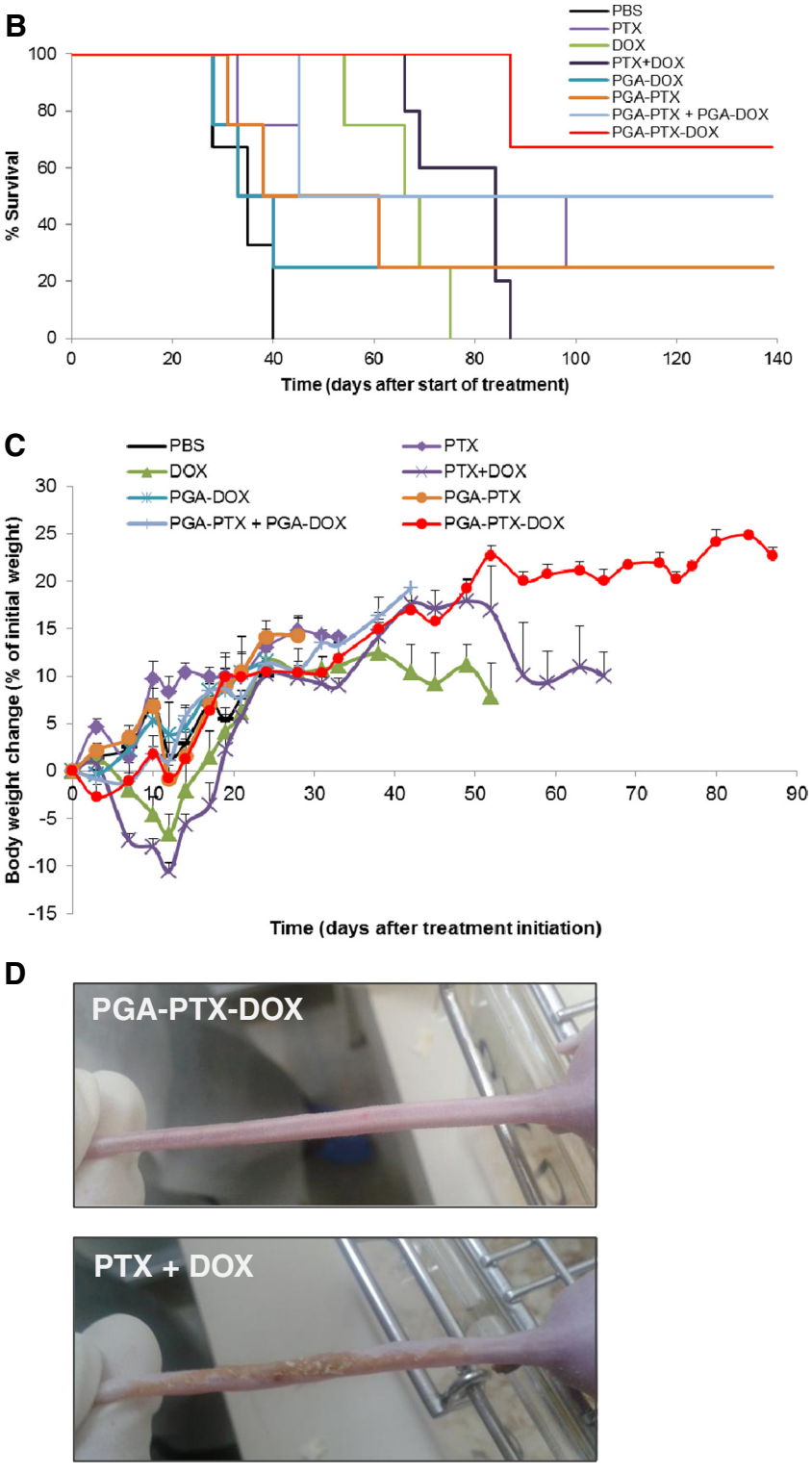

Fig. 9 (*continued*).

unexpectedly it did not induce any tumor growth inhibition *in vivo* compared to PBS-treated mice (T/C = 1.05). However, when combined with PGA–PTX ((T/C = 0.55), PGA–DOX did improve its anticancer efficacy when treating the same tumor-bearing mice (T/C = 0.38), indicating a synergistic effect.

The superiority of the conjugate is evident in its safety compared to free drugs, especially to DOX and PTX plus DOX groups that suffered from extreme weight loss, immediately following the treatments and also several weeks later. Those treatments caused a reduction of up to 15% in body weight, whereas treatment with the conjugates at equivalent concentrations did not. Free DOX was more toxic than free PTX, since it was given at a higher dose and the highest toxicity was observed in the PTX plus DOX-treated group of mice. It is known from previous studied that PGA alone is non-toxic at the relevant concentrations used in our experiments [21]. Our work provides *in vivo* evidence for the potential of polymer-based multi-drug targeting and strengthens its prospective clinical translation based on systematically- and rationally-designed combinations.

Table 3
Tumor/control ratio at day 26 following treatment initiation.

	PBS	PTX	DOX	PTX + DOX	PGA–DOX	PGA–PTX	PGA–DOX + PGA–PTX	PGA–PTX–DOX
T/C ratio	1	0.3	0.19	0.19	1.05	0.55	0.38	0.08

5. Conclusions

We demonstrated a concept of a combined polymer therapeutic designed to target breast and ovarian cancer by co-delivery of two synergistic drugs conjugated to a single polymer chain. PGA–PTX–DOX nano-conjugate was synthesized and evaluated *in vitro* and *in vivo*, and was found to be a highly active and non-toxic antitumor agent. Conjugation with PGA allowed PTX to be soluble in water, as opposed to free PTX. PGA–PTX–DOX exhibited a significant anti-proliferative and anti-migratory effect on MDA-MB-231 and ES-2 cells. More importantly, our novel conjugate was highly effective in inhibiting the growth of mammary tumors, compared to a combination of free drugs and drugs conjugated to polymers separately. In addition, the conjugate showed improved safety profile compared to the free drugs. Conjugation of chemotherapeutic drugs to PGA allows specific delivery to the tumor by the EPR effect and provides an ideal platform for true combination therapy, since both drugs are given simultaneously in one injection and share the same pharmacokinetic profile.

Supplementary data to this article can be found online at http://dx.doi.org/10.1016/j.jconrel.2014.05.025.

Acknowledgments

This study was partially supported by The European Research Council (ERC) Consolidator Award (617445—PolyDorm), The Israel Science Foundation (Grant No. 1309/10), the Swiss Bridge Award, and by grants from the Israeli National Nanotechnology Initiative (INNI), Focal Technology Area (FTA) program: Nanomedicine for Personalized Theranostics, and by The Leona M. and Harry B. Helmsley Nanotechnology Research Fund.

References

[1] Y. Matsumura, H. Maeda, A new concept for macromolecular therapeutics in cancer chemotherapy: mechanism of tumoritropic accumulation of proteins and the antitumor agent smancs, Cancer Res. 46 (1986) 6387–6392.
[2] H. Maeda, J. Wu, T. Sawa, Y. Matsumura, K. Hori, Tumor vascular permeability and the EPR effect in macromolecular therapeutics: a review, J Control Release 65 (2000) 271–284.
[3] E. Markovsky, H. Baabur-Cohen, A. Eldar-Boock, L. Omer, G. Tiram, S. Ferber, P. Ofek, D. Polyak, A. Scomparin, R. Satchi-Fainaro, Administration, distribution, metabolism and elimination of polymer therapeutics, J. Control. Release 161 (2012) 446–460.
[4] H. Maeda, H. Nakamura, J. Fang, The EPR effect for macromolecular drug delivery to solid tumors: improvement of tumor uptake, lowering of systemic toxicity, and distinct tumor imaging *in vivo*, Adv. Drug Deliv. Rev. 65 (2013) 71–79.
[5] D. Polyak, A. Eldar-Boock, H. Baabur-Cohen, R. Satchi-Fainaro, Polymer conjugates for focal and targeted delivery of drugs, Polym. Adv. Technol. 24 (2013) 777–790.
[6] R. Duncan, M.J. Vicent, Polymer therapeutics—prospects for 21st century: the end of the beginning, Adv. Drug Deliv. Rev. 65 (2013) 60–70.
[7] J. Kopecek, P. Kopeckova, T. Minko, Z.R. Lu, C.M. Peterson, Water soluble polymers in tumor targeted delivery, J. Control. Release 74 (2001) 147–158.
[8] J. Kopecek, Polymer–drug conjugates: origins, progress to date and future directions, Adv. Drug Deliv. Rev. 65 (2013) 49–59.
[9] F. Greco, M.J. Vicent, Combination therapy: opportunities and challenges for polymer–drug conjugates as anticancer nanomedicines, Adv. Drug Deliv. Rev. 61 (2009) 1203–1213.
[10] F. Kratz, A. Warnecke, Finding the optimal balance: challenges of improving conventional cancer chemotherapy using suitable combinations with nano-sized drug delivery systems, J. Control. Release 164 (2012) 221–235.
[11] A. Eldar-Boock, D. Polyak, A. Scomparin, R. Satchi-Fainaro, Nano-sized polymers and liposomes designed to deliver combination therapy for cancer, Curr. Opin. Biotechnol. 24 (2013) 682–689.
[12] S.G. Arbuck, Taxol (paclitaxel): future directions, Ann. Oncol. 5 (Suppl. 6) (1994) S59–S62.
[13] R.B. Weiss, The anthracyclines: will we ever find a better doxorubicin? Semin. Oncol. 19 (1992) 670–686.
[14] C. Jin, H. Li, Y. He, M. He, L. Bai, Y. Cao, W. Song, K. Dou, Combination chemotherapy of doxorubicin and paclitaxel for hepatocellular carcinoma *in vitro* and *in vivo*, J. Cancer Res. Clin. Oncol. 136 (2010) 267–274.
[15] H. Wang, Y. Zhao, Y. Wu, Y.L. Hu, K. Nan, G. Nie, H. Chen, Enhanced anti-tumor efficacy by co-delivery of doxorubicin and paclitaxel with amphiphilic methoxy PEG–PLGA copolymer nanoparticles, Biomaterials 32 (2011) 8281–8290.
[16] J. Jassem, T. Pienkowski, A. Pluzanska, S. Jelic, V. Gorbunova, J. Berzins, T. Nagykalnai, L. Biganzoli, A. Aloe, L. Astier, S. Munier, Doxorubicin and paclitaxel versus fluorouracil, doxorubicin and cyclophosphamide as first-line therapy for women with advanced breast cancer: long-term analysis of the previously published trial, Onkologie 32 (2009) 468–472.
[17] J. Jassem, T. Pienkowski, A. Pluzanska, S. Jelic, V. Gorbunova, Z. Mrsic-Krmpotic, J. Berzins, T. Nagykalnai, N. Wigler, J. Renard, S. Munier, C. Weil, Doxorubicin and paclitaxel versus fluorouracil, doxorubicin, and cyclophosphamide as first-line therapy for women with metastatic breast cancer: final results of a randomized phase III multicenter trial, J. Clin. Oncol. 19 (2001) 1707–1715.
[18] L. Gianni, E.H. Herman, S.E. Lipshultz, G. Minotti, N. Sarvazyan, D.B. Sawyer, Anthracycline cardiotoxicity: from bench to bedside, J. Clin. Oncol. 26 (2008) 3777–3784.
[19] H. Gelderblom, J. Verweij, K. Nooter, A. Sparreboom, Cremophor EL: the drawbacks and advantages of vehicle selection for drug formulation, Eur. J. Cancer 37 (2001) 1590–1598.
[20] J.M. Buescher, A. Margaritis, Microbial biosynthesis of polyglutamic acid biopolymer and applications in the biopharmaceutical, biomedical and food industries, Crit. Rev. Biotechnol. 27 (2007) 1–19.
[21] A. Eldar-Boock, K. Miller, J. Sanchis, R. Lupu, M.J. Vicent, R. Satchi-Fainaro, Integrin-assisted drug delivery of nano-scaled polymer therapeutics bearing paclitaxel, Biomaterials 32 (2011) 3862–3874.
[22] C. Li, Poly(L-glutamic acid)–anticancer drug conjugates, Adv. Drug Deliv. Rev. 54 (2002) 695–713.
[23] T. Strojnik, I. Zajc, A. Bervar, B. Zidanik, R. Golouh, J. Kos, V. Dolenc, T. Lah, Cathepsin B and its inhibitor stefin A in brain tumors, Pflugers Arch. 439 (2000) R122–R123.
[24] T. Strojnik, J. Kos, B. Zidanik, R. Golouh, T. Lah, Cathepsin B immunohistochemical staining in tumor and endothelial cells is a new prognostic factor for survival in patients with brain tumors, Clin. Cancer Res. 5 (1999) 559–567.
[25] J. Decock, N. Obermajer, S. Vozelj, W. Hendrickx, R. Paridaens, J. Kos, Cathepsin B, cathepsin H, cathepsin X and cystatin C in sera of patients with early-stage and inflammatory breast cancer, Int. J. Biol. Markers 23 (2008) 161–168.
[26] J.A. Foekens, J. Kos, H.A. Peters, M. Krasovec, M.P. Look, N. Cimerman, M.E. Meijer-van Gelder, S.C. Henzen-Logmans, W.L. van Putten, J.G. Klijn, Prognostic significance of cathepsins B and L in primary human breast cancer, J. Clin. Oncol. 16 (1998) 1013–1021.
[27] M. Markman, Improving the toxicity profile of chemotherapy for advanced ovarian cancer: a potential role for CT-2103, J. Exp. Ther. Oncol. 4 (2004) 131–136.
[28] V.L. Galic, J.D. Wright, S.N. Lewin, T.J. Herzog, Paclitaxel poliglumex for ovarian cancer, Expert Opin. Investig. Drugs 20 (2011) 813–821.
[29] C.J. Langer, K.J. O'Byrne, M.A. Socinski, S.M. Mikhailov, K. Lesniewski-Kmak, M. Smakal, T.E. Ciuleanu, S.V. Orlov, M. Dediu, D. Heigener, A.J. Eisenfeld, L. Sandalic, F.B. Oldham, J.W. Singer, H.J. Ross, Phase III trial comparing paclitaxel poliglumex (CT-2103, PPX) in combination with carboplatin versus standard paclitaxel and carboplatin in the treatment of PS 2 patients with chemotherapy-naive advanced non-small cell lung cancer, J. Thorac. Oncol. 3 (2008) 623–630.
[30] S. Jeyapalan, J. Boxerman, J. Donahue, M. Goldman, T. Kinsella, T. Dipetrillo, D. Evans, H. Elinzano, M. Constantinou, E. Stopa, Y. Puthawala, D. Cielo, A. Santaniello, A. Oyelese, K. Mantripragada, K. Rosati, D. Isdale, H. Safran, Paclitaxel poliglumex, temozolomide, and radiation for newly diagnosed high-grade glioma: a Brown University Oncology Group Study, Am. J. Clin. Oncol. (2013), http://dx.doi.org/10.1097/COC.0b013e31827de92b [in press].
[31] M.J. Vicent, F. Greco, R.I. Nicholson, A. Paul, P.C. Griffiths, R. Duncan, Polymer therapeutics designed for a combination therapy of hormone-dependent cancer, Angew. Chem. Int. Ed. Engl. 44 (2005) 4061–4066.
[32] T. Lammers, V. Subr, K. Ulbrich, P. Peschke, P.E. Huber, W.E. Hennink, G. Storm, Simultaneous delivery of doxorubicin and gemcitabine to tumors *in vivo* using prototypic polymeric drug carriers, Biomaterials 30 (2009) 3466–3475.
[33] A. Ponta, Y. Bae, PEG–poly(amino acid) block copolymer micelles for tunable drug release, Pharm. Res. 27 (2010) 2330–2342.
[34] W. Song, Z. Tang, M. Li, S. Lv, H. Sun, M. Deng, H. Liu, X. Chen, Polypeptide-based combination of paclitaxel and cisplatin for enhanced chemotherapy efficacy and reduced side-effects, Acta Biomater. 10 (2014) 1392–1402.
[35] Y. Zhou, J. Yang, J.S. Rhim, J. Kopecek, HPMA copolymer-based combination therapy toxic to both prostate cancer stem/progenitor cells and differentiated cells induces durable anti-tumor effects, J. Control. Release 172 (2013) 946–953.
[36] G. Bulaj, T. Kortemme, D.P. Goldenberg, Ionization–reactivity relationships for cysteine thiols in polypeptides, Biochemistry 37 (1998) 8965–8972.
[37] D. Willner, P.A. Trail, S.J. Hofstead, H.D. King, S.J. Lasch, G.R. Braslawsky, R.S. Greenfield, T. Kaneko, R.A. Firestone, 6-Maleimidocaproyl)hydrazone of doxorubicin—a new derivative for the preparation of immunoconjugates of doxorubicin, Bioconjug. Chem. 4 (1993) 521–527.
[38] T.C. Chou, Drug combination studies and their synergy quantification using the Chou–Talalay method, Cancer Res. 70 (2010) 440–446.

[39] F. Greco, M.J. Vicent, S. Gee, A.T. Jones, J. Gee, R.I. Nicholson, R. Duncan, Investigating the mechanism of enhanced cytotoxicity of HPMA copolymer–Dox–AGM in breast cancer cells, J. Control. Release 117 (2007) 28–39.
[40] Y. Bae, T.A. Diezi, A. Zhao, G.S. Kwon, Mixed polymeric micelles for combination cancer chemotherapy through the concurrent delivery of multiple chemotherapeutic agents, J. Control. Release 122 (2007) 324–330.
[41] F. Ahmed, R.I. Pakunlu, A. Brannan, F. Bates, T. Minko, D.E. Discher, Biodegradable polymersomes loaded with both paclitaxel and doxorubicin permeate and shrink tumors, inducing apoptosis in proportion to accumulated drug, J. Control. Release 116 (2006) 150–158.
[42] C. Li, R.A. Newman, Q.P. Wu, S. Ke, W. Chen, T. Hutto, Z. Kan, M.D. Brannan, C. Charnsangavej, S. Wallace, Biodistribution of paclitaxel and poly(L-glutamic acid)–paclitaxel conjugate in mice with ovarian OCa-1 tumor, Cancer Chemother. Pharmacol. 46 (2000) 416–422.
[43] V. Omelyanenko, P. Kopeckova, C. Gentry, J. Kopecek, Targetable HPMA copolymer–adriamycin conjugates. Recognition, internalization, and subcellular fate, J. Control. Release 53 (1998) 25–37.
[44] P.S. Lai, P.J. Lou, C.L. Peng, C.L. Pai, W.N. Yen, M.Y. Huang, T.H. Young, M.J. Shieh, Doxorubicin delivery by polyamidoamine dendrimer conjugation and photochemical internalization for cancer therapy, J. Control. Release 122 (2007) 39–46.
[45] D. Belotti, M. Rieppi, M.I. Nicoletti, A.M. Casazza, T. Fojo, G. Taraboletti, R. Giavazzi, Paclitaxel (Taxol(R)) inhibits motility of paclitaxel-resistant human ovarian carcinoma cells, Clin. Cancer Res. 2 (1996) 1725–1730.
[46] D.I. Axel, W. Kunert, C. Goggelmann, M. Oberhoff, C. Herdeg, A. Kuttner, D.H. Wild, B. R. Brehm, R. Riessen, G. Koveker, K.R. Karsch, Paclitaxel inhibits arterial smooth muscle cell proliferation and migration *in vitro* and *in vivo* using local drug delivery, Circulation 96 (1997) 636–645.
[47] K. Miller, R. Erez, E. Segal, D. Shabat, R. Satchi-Fainaro, Targeting bone metastases with a bispecific anticancer and antiangiogenic polymer–alendronate–taxane conjugate, Angew. Chem. Int. Ed. Engl. 48 (2009) 2949–2954.
[48] D. Landesman-Milo, M. Goldsmith, S. Leviatan Ben-Arye, B. Witenberg, E. Brown, S. Leibovitch, S. Azriel, S. Tabak, V. Morad, D. Peer, Hyaluronan grafted lipid-based nanoparticles as RNAi carriers for cancer cells, Cancer Lett. 334 (2013) 221–227.
[49] S.M. Moghimi, Mechanisms of splenic clearance of blood cells and particles: towards development of new splenotropic agents, Adv. Drug Deliv. Rev. 17 (1995) 103–115.